High-T_c superconductivity in doped boron-carbon clathrates

Simone Di Cataldo,[1,2] Shadi Qulaghasi,[1,*] Giovanni B. Bachelet,[1,3] and Lilia Boeri[1,3,†]
[1]*Dipartimento di Fisica, Sapienza Università di Roma, 00185 Roma, Italy*
[2]*Institute of Theoretical and Computational Physics, Graz University of Technology, NAWI Graz, 8010 Graz, Austria*
[3]*Centro Ricerche Enrico Fermi, Via Panisperna, 89a, 00184 Roma, Italy*

(Received 11 October 2021; accepted 7 February 2022; published 25 February 2022)

We report a high-throughput *ab initio* study of the thermodynamic and superconducting properties of the recently synthesized XB_3C_3 clathrates. These compounds, in which boron and carbon form a spongelike network of interconnected cages each enclosing a central X atom, are attractive candidates to achieve high-T_c conventional superconductivity at ambient pressure, due to the simultaneous presence of a stiff B-C covalent network and a tunable Fermi energy due to the X atom acting as a charge reservoir. Ternary compounds like CaB_3C_3, SrB_3C_3, and BaB_3C_3 are predicted to exhibit $T_c \lesssim 50$ K at moderate or ambient pressures, which may further increase up to 77 K if the original compounds are hole doped, by replacing the divalent alkaline earth with a monovalent alkali metal to form an ordered XYB_6C_6 alloy.

DOI: 10.1103/PhysRevB.105.064516

I. INTRODUCTION

More than one century after its discovery [1], the *hydride rush* initiated by the report of a superconducting critical temperature (T_c) of 203 K in SH_3 [2,3] completely reshaped the landscape of research on superconductivity, delivering the first example, at the same time, of room-temperature superconductivity and of predictive materials science based on computational methods [4–10].

The focus of the field is gradually shifting from achieving ever larger T_c's to finding new high-T_c materials which can operate at (or close to) ambient pressure. Migdal-Eliashberg theory for superconductivity suggests that, besides hydrides [11,12], obvious candidates for observing high-T_c superconductivity from conventional (electron-phonon, hereafter *e-ph*) interaction are light-element compounds. In particular, boron and/or carbon compounds combine large phonon frequencies and covalent bonds, the two most important ingredients underlying high-T_c (conventional) superconductivity [13–15]. Several theoretical predictions of conceivable high-T_c borides and carbides date back to the early 2000's, but none of them has been experimentally verified [16–20]. Twenty years later, the problem is being revisited with modern *ab initio* methods for structural prediction, which permit us to address the thermodynamic stability of different structures across the phase diagram [21,22]. Last year, Zhu *et al.* [23] reported the formation of a previously unknown boron-carbon phase, with chemical formula XB_3C_3, which is a structural analog of high-T_c sodalite clathrate hydrides, like LaH_{10}, YH_6, etc. [24–29]. The structure, shown in Fig. 1, consists of a bcc lattice of interconnected *truncated octahedral* boron-carbon cages, each enclosing a guest X atom.

While the *empty* B-C cage is dynamically and thermodynamically unstable at ambient pressure, a few XB_3C_3 compounds can be stabilized under pressure and exhibit a variety of attractive physical properties, such as superhardness (La) and ferroelectricity (Sc) [23,30,31]. Among them SrB_3C_3, which forms in diamond anvil cells at high pressure (57 GPa) but survives close to room pressure, has been theoretically predicted to superconduct below 40 K [32,33], a T_c close to the current record for ambient-pressure conventional superconductivity, held by magnesium diboride (MgB_2) [13]. Given the extreme versatility of cagelike structures observed in superhydrides, we expect that a suitable choice of the guest atom is likely to attain even higher T_c. In this paper we explore such a possibility by performing a detailed study of thermodynamic and superconducting properties of B-C clathrates, using first-principles methods based on density functional theory (DFT) [34].

Our sampling of conceivable compositions starts from a scan of the first 57 elements $Z = 1$–57. We estimate the dynamical and thermodynamic stability of XB_3C_3 compounds with $X =$ H-La, and find that only five (Ca, Sr,Y, Ba, La) form stable XB_3C_3 compounds, but none of them represents a substantial improvement over MgB_2 in terms of T_c and thermodynamic stability.

We then consider the possibility of combining pairs of mono- and divalent elements to optimize the electronic properties in the direction of a higher T_c, and find several ordered alloys XYB_6C_6 which should exhibit critical temperatures at the liquid-nitrogen boiling point. These compounds form under pressure, but may be quenched down to room pressure without losing their remarkable properties. We argue that a further fine tuning of the doping level is very likely to further enhance T_c and reduce the stabilization pressure.

II. COMPUTATIONAL DETAILS

Our calculations, based on the density functional theory, were performed using Quantum Espresso (QE) [35,36], scalar-relativistic optimized norm-conserving Vanderbilt

*ArcelorMittal SA, 24 Bd d'Avranches - 1160, Luxembourg.
†lilia.boeri@uniroma1.it

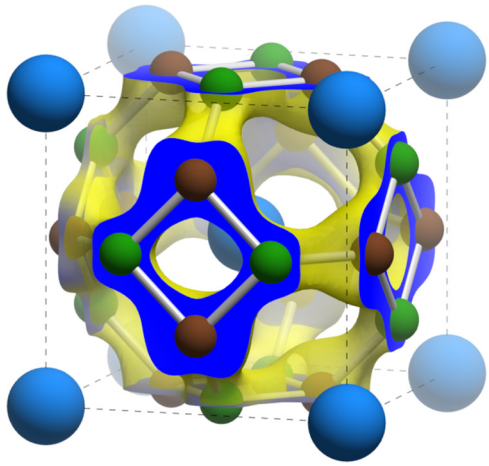

FIG. 1. Crystal structure of $X\mathrm{B_3C_3}$. Space group: $Pm\bar{3}n$ (223); large blue, small brown, and green spheres indicate X, B, and C atoms, in Wyckoff positions $2a$, $6d$, and $6c$, respectively. The yellow isosurface, obtained for X = Sr but representative of the valence-band-top wave function for all the $X\mathrm{B_3C_3}$ compounds considered in this work (see also Fig. 3), closely wraps the network of B-C bonds (see text); electric-blue lamellas mark its cross section at the cell boundaries.

pseudopotentials [37], and a Perdew-Burke-Ernzerhof exchange-correlation functional [38]. The wave functions were expanded using a plane-wave basis set, with a cutoff of 80 Ry. The integration over the Brillouin zone was performed on a $6 \times 6 \times 6$ $\vec{k}$-space grid, using a Methfessel-Paxton [39] smearing width of 0.06 Ry. Such a choice ensures a 0.5 meV/atom convergence of the total energy and a 0.5 meV convergence of the phonon frequencies.

The dynamical matrices and the related *e-ph* matrix elements were calculated using linear response theory [40]. The Brillouin zone was sampled on a $4 \times 4 \times 4$ $\vec{q}$-grid (phonons), and the integration of the *e-ph* matrix elements was carried out on a $30 \times 30 \times 30$ $\vec{k}$-grid (electrons) and a Gaussian smearing width of 200 meV. The superconducting critical temperature was estimated by numerically solving the isotropic Éliashberg equations employing the Éliashberg functions obtained in linear response.

III. HIGH-THROUGHPUT STUDY OF $X\mathrm{B_3C_3}$ CLATHRATE STABILITY

The main results of our initial high-throughput screening are summarized in Fig. 2 [34]. For each of the first 57 elements of the periodic table (X = H-La), we performed a full relaxation of the $X\mathrm{B_3C_3}$ structure at ambient pressure. For the relaxed structures we computed the decomposition enthalpy with respect to the ground-state elemental structures $\Delta H = H(X\mathrm{B_3C_3}) - H(X) - 3H(\mathrm{B}) - 3H(\mathrm{C})$, where $H(X\mathrm{B_3C_3})$ is the enthalpy of the $X\mathrm{B_3C_3}$ structure relaxed at a given pressure, and $H(X)$, $H(\mathrm{B})$, and $H(\mathrm{C})$ are the enthalpies of the three elements in their ground-state structure at the same pressure [41]. This quantity is shown on a per atom basis in Fig. 2; a comparison between $\Delta H(P = 0\ \mathrm{GPa})$ and $\Delta H(P = 50\ \mathrm{GPa})$ is shown in Fig. S1 of the Supplemental Material [42].

Note that the decomposition enthalpy ΔH thus defined only provides a lower bound on the actual formation enthalpy. The latter also includes the decomposition into all possible binary and ternary phases on the hull, which is unfeasible in a high-throughput study. However, a negative $\Delta H(P)$ usually indicates that the phase will survive down to pressure P, if formed at higher pressure.

In our scan, only Ca, Y, and La are predicted to remain stable down to ambient pressure; and, indeed, $\mathrm{LaB_3C_3}$ has been experimentally reported to form at 1 atm [31].

The green-shaded region in Fig. 2 indicates the range of *metastability*, i.e., an energy region with $\Delta H > 0$, which encloses structures that may be synthesized under appropriate experimental conditions. Although there is no rigorous criterion for metastability, values of ΔH ranging from a few tens to a few hundreds meV are considered acceptable in literature [43]; here we choose $\Delta H = 250$ meV, roughly corresponding to the average pV term at 50 GPa.

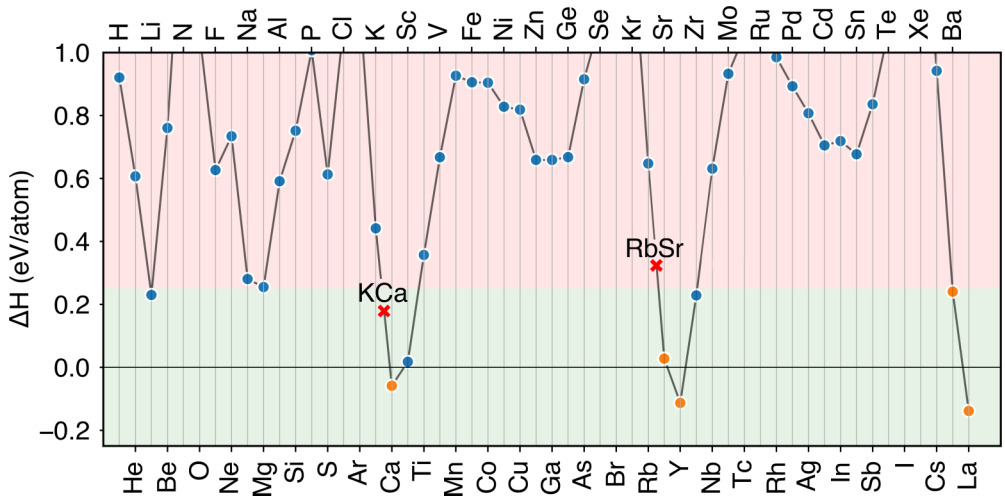

FIG. 2. Decomposition enthalpy of $X\mathrm{B_3C_3}$ compounds for the first 57 elements of the periodic table (Z = 1–57; the chemical symbol is shown above for odd-Z elements, below for even-Z elements). The color of markers relates to dynamical stability: blue dots indicate dynamically unstable compounds, and orange dots dynamically stable ones. All quantities are calculated at $P = 0$.

In addition to thermodynamic stability, Fig. 2 includes information on the *dynamical* (phonon) stability of XB_3C_3 compounds, estimated from linear-response calculations on a 2^3 grid in reciprocal space [34]. Compounds marked with orange symbols have real frequencies on all grid points, while blue symbols highlight the presence of at least one imaginary frequency, and hence a dynamical instability. Our criterion correctly classifies ferroelectric ScB_3C_3 as dynamically unstable [30].

A first inspection of the figure reveals that the formation of XB_3C_3 structures is energetically unfavorable for most elements in the periodic table; only three elements have negative decomposition enthalpies. Interestingly, all three compounds are predicted to be also *dynamically* stable, which is a strong indication that they may be synthesised, under appropriate conditions. In addition to the thermodynamically stable compounds at zero pressure, two more compounds, SrB_3C_3 and BaB_3C_3, which have a positive decomposition enthalpy at ambient pressure, can be stabilized at higher pressure. The decomposition pressures (P_d), estimated by linear interpolation of the decomposition enthalpies between 0 and 50 GPa, are 5 and 30 GPa in Sr and Ba, respectively. The corresponding formation pressures are expected to be significantly higher: for SrB_3C_3, where experimental data are available [23], the difference between the decomposition pressure and the measured formation pressure is ∼50 GPa. Assuming a similar shift, the formation pressure of BaB_3C_3 could be as high as 80 GPa.

The five elements which form stable XB_3C_3 compounds (i.e., Ca, Sr, Y, Ba, La) all belong either to the II A or to the III A group of the periodic table. An inspection of their electronic structure and structural data reveals that these elements lie in a sweet spot of valence and atomic radius; moreover, their low electronegativity implies that, within the B-C cage, they are completely ionized: their valence states do not mix with B-C states, and thus do not disrupt the stability of the structure. The (weak) dependence of the lattice parameter on the X atom is shown in Fig. S2 of the Supplemental Material [42].

IV. ELECTRONS AND PHONONS

Figure 3 shows a magnification of the electronic band structure near the Fermi level of the five dynamically stable compounds at ambient pressure and their immediate neighbors in the periodic table, arranged by period (K, Ca, Sc; Rb, Sr, Y; Cs, Ba, La) [44]. For each compound, the energy zero is chosen in such a way as to coincide with the top of its valence bands; the position of the Fermi levels is shown as a blue dashed line. Such a choice stresses that the electronic bands of XB_3C_3, with X belonging to the same period or group, follow a rigid-band model: in the valence region they are of almost pure B-C character; the guest X atoms, almost completely ionized, donate their charge to the sublattice of B-C cages, filling its bands. As a result, when X is one of the trivalent elements Y or La, XB_3C_3 is insulating: its 24 valence electrons exactly fill up the 12 mostly B-C bonding bands, separated by a ∼1 eV gap from the conduction bands (where, instead, antibonding B-C and X guest states do mix); not so with Sc, upper right panel of Fig. 3, because its empty d states drop so low in energy that they partially hybridize with the top of the valence bands, yielding a poor metal.

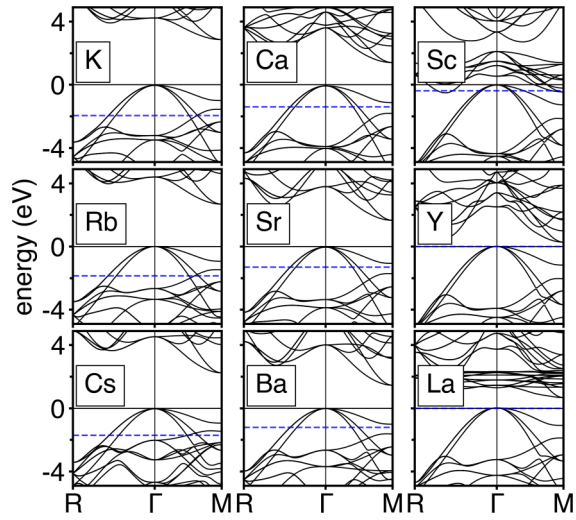

FIG. 3. Band structure of nine XB_3C_3 compounds. The energy zero is equal to the valence band tops; the Fermi energy is a blue horizontal dashed line. See text.

Replacing tri- with di- and monovalent elements (middle and left panels of Fig. 3, respectively), the Fermi level is shifted into the valence band, effectively doping it with holes. In Fig. 1 we show the XB_3C_3 crystal structure where the yellow surface is the isosurface corresponding to one fourth of the maximum value of the square modulus of the valence-band-top wave function [45]. Such an isosurface, obtained for X = Sr but representative of all the XB_3C_3 compounds appearing in Fig. 3, closely wraps the network of B-C bonds. Holes doped into this band will experience a very strong *e-ph* coupling to bond-stretching phonons; a similar mechanism is at the heart of the remarkable superconducting properties of other B-C compounds, such as MgB_2, boron-doped diamond, graphane [13,15,19,20,22,46]. In XB_3C_3 this very mechanism leads to substantial T_c's. For metallic structures, using linear-response *e-ph* spectra and the McMillan-Allen-Dynes formula, assuming $\mu^* = 0.1$, we predict T_c values between 40 and 50 K– see Table I. Calculations are performed at zero pressure, where all compounds are dynamically stable, although Ca has a very soft mode along the Γ-M line. In all cases, the *e-ph* spectra (available in Figs. S3 to S8 of the Supplemental Material [42]) are very similar to those shown for the doped sample of Fig. 5: the phonon frequencies extend

TABLE I. Calculated superconducting properties of stable XB_3C_3 compounds; the asterisk indicates that in CaB_3C_3 one of the optical phonons between M and Γ experiences a remarkable softening.

	P_d (GPa)	$\Delta H_{P=0}$ (meV/atom)	$\omega_{\log}$ (meV)	λ	T_c (K)
Ca	0	−59	17.5*	1.9	48
Sr	0	+28	51.0	1.0	44
Ba	30	+234	49.8	1.1	50

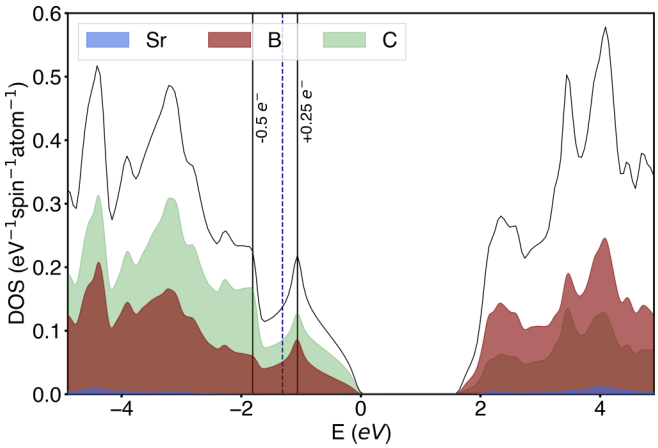

FIG. 4. Electronic density of states of SrB_3C_3 near the Fermi level (vertical dashed line). See text.

up to ∼100 meV and the *e-ph* coupling is spread over a wide range of frequencies, with a strong enhancement in the mid-frequency region where softer bond-stretching phonons are concentrated.

V. DOPING

The rigid-band behavior observed in Fig. 3 suggests that a partial substitution at the guest site may be used to improve the superconducting properties of alkaline-earth BC–clathrates. We start from atoms belonging to the same row of the periodic table (and of Fig. 3), whose substitution should be easiest on geometrical and chemical grounds. In Fig. 4 the magnification of the electronic density of states (DOS) around the Fermi level, which in SrB_3C_3 lies more than 1 eV below the top of the valence bands, emphasizes its position (marked by a vertical dashed line) within a ∼1 eV wide pseudogap, which clearly separates a left-hand DOS shoulder, corresponding to a 1/2 hole/f.u. doping, from an equally tall right-hand sharp peak, corresponding to a 1/4 electron doping (both marked by vertical solid lines). While a 1/4 electron doping requires a large supercell, a 1/2 hole doping may be easily simulated

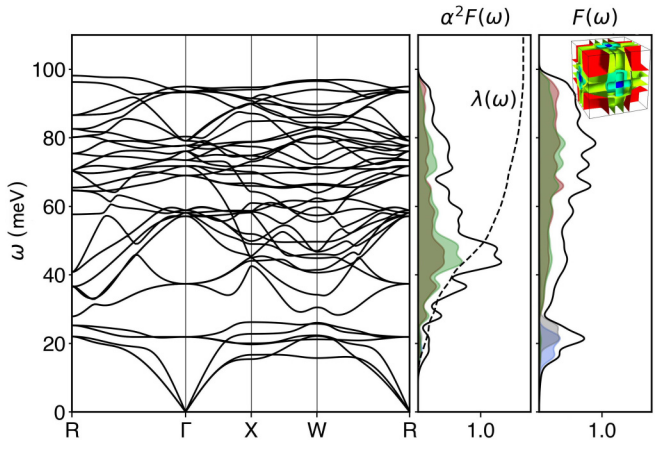

FIG. 5. Phonon dispersions (left), density of states (middle), Eliashberg spectral function and Fermi surface (right) of $RbSrB_6C_6$ (T_c = 77 K). Projections on the host B and C atoms are shown in green and brown, respectively; on the guest atoms, in blue.

TABLE II. Predicted thermodynamic and superconducting properties of ordered alloys XYB_6C_6; quantities are defined as in Table I. The asterisk reminds that for CsBa the superconducting parameters were calculated at P = 10 GPa (see text). In the last row we report data for 50% B-doped diamond, from Ref. [22]. Note that, in that paper, T_c was estimated by the Mc-Millan-Allen-Dynes formula, while in the present work we employ the full solution of Migdal-Eliashberg equations, which is more accurate at strong coupling.

	P ($\Delta H = 0$) (GPa)	ΔH ($P = 0$) (meV/atom)	$\omega_{\log}$ (meV)	λ	T_c (K)
KCa	20	+178	43.9	1.6	77
RbSr	42	+324	44.0	1.7	78
CsBa	109	+578	35.4*	2.2*	82*
NaSr	18	+153	34.4	2.1	80
B-diamond [22]	–	+440	41.0	2.3	75

by a simple cubic supercell, in which half of the divalent Sr atoms are replaced by monovalent Rb atoms. At ambient pressure, such an ordered alloy is 12 meV/atom more stable than isolated SrB_3C_3 + isolated RbB_3C_3, but its decomposition enthalpy with respect to the pure elements is high: ΔH = 324 meV/atom. In analogy to SrB_3C_3, we expect that, at higher pressure, ΔH is reduced and $RbSrB_6C_6$ becomes stable. Following this line of reasoning, the estimated decomposition pressure for $RbSrB_6C_6$ would be P_d = 42 GPa.

Since the rigid-band behavior of Fig. 3 not only implies an almost identical electronic DOS, but also, at equal band filling, has the consequence of a very similar phonon DOS and thus T_c, we decided that, in addition to $RbSrB_6C_6$, also the second- and fourth-row compounds $KCaB_6C_6$ and $CsBaB_6C_6$, respectively obtained by doping CaB_3C_3 and BaB_3C_3 with same-row monovalent atoms K and Cs, deserve detailed investigation, and for them we predict decomposition pressures of 20 and 109 GPa, which, within the small set of compounds considered, suggests that smaller average ionic radii yield lower decomposition pressures—see Table II.

Figure 5 shows the calculated phonon dispersions and density of states of $RbSrB_6C_6$, together with the *e-ph* Eliashberg spectral function $\alpha^2F(\omega)$. Analogous figures for $KCaB_6C_6$ and $CsBaB_6C_6$ may be found in the Supplemental Material [42]. The *e-ph* coupling is mostly distributed on modes of the B-C host sublattice; a strong enhancement in their mid-frequency range, where soft bond-stretching phonons are concentrated, translates into relatively low $\omega_{\log}$ (∼44 meV), and very large *e-ph* coupling constant λ = 1.7. Given the strong-coupling regime, we estimated the superconducting critical temperature by solving the full (isotropic) Migdal-Eliashberg equations, obtaining, with constant $\mu^* = 0.1$, T_c = 77 K.

Table II reports the relevant superconducting parameters for the other two ordered alloys considered here. The quantities calculated at ambient pressure for $KCaB_6C_6$ are very close to those estimated for $RbSrB_6C_6$. The results reported for $CsBaB_6C_6$, which proves weakly dynamically unstable at ambient pressure, are taken at 10 GPa; here the predicted T_c = 82 K is slightly larger than the liquid-nitrogen boiling point. Table II confirms that in these compounds the *e-ph* coupling mainly comes from the B-C bonds: while the guest radius has

a major impact on pressure, its effect on T_c appears almost negligible.

In an attempt to further reduce the formation pressure, we also considered the possibility of mixing mono- and divalent elements belonging to different rows of the periodic table (inter-row doping), while keeping the (optimal) average valency of $Z_v = 1.5$. We computed the electronic and vibrational properties of XYB_6C_6 obtained from all combinations of X = (Na,K,Rb,Cs), Y = (Ca,Sr,Ba) atoms.

As shown in Fig. S9 of the Supplemental Material, electronic and vibrational spectra are almost identical for all XYB_6C_6 compounds thus obtained, indicating that the rigid-band model remains valid for inter-row doping [47]. Thermodynamic and dynamical stability, on the other hand, strongly depend on the average atomic radius of the (X, Y) pair: out of all the inter-row combinations considered here, only $NaSrB_6C_6$, $KSrB_6C_6$, and $RbCaB_6C_6$ turn out to be dynamically stable. $NaSrB_6C_6$ is predicted to have a lower formation enthalpy and stabilization pressure than our best same-row candidate $KCaB_6C_6$ (see Fig. S10 of the Supplemental Material). For this compound, as reported in the last row of Table II, we computed a T_c of 86 K.

The data reported in Table II suggest that doped XB_3C_3 compounds represent a substantial step forward in our understanding of conventional superconductors. Critical temperatures close to or larger than the liquid-nitrogen boiling point (77 K) have never been reported in any conventional superconductor at room pressure; at this pressure the current record is much lower—-about half of it, $T_c = 39$ K in MgB_2. In the last row of Table II we report the data corresponding to heavily (50%) B-doped diamond, also predicted to exhibit a T_c close to 80 K [19,22]. Its main superconducting parameters are remarkably close, which suggests that lattice stiffness, bonding properties, nature, and distribution of the *e-ph* coupling are similar to those of the XB_3C_3 structures. The key difference is that, in heavily B-doped diamond, ΔH is so high (∼440 meV) that its experimental synthesis is probably impossible (the highest reported B-doping levels in diamond are 4–5 times smaller), while, according to our calculations, $KCaB_3C_3$ and $NaSrB_3C_3$, just like SrB_3C_3, are likely to form at relatively low pressure, and then, once formed, to be quenched down to ambient pressure, without spoiling their substantial T_c. In addition (i) the empirical correlation between average guest radius and stabilization pressure, (ii) the rigid-band behavior for both intra- and inter-row substitution (Fig. 3, and Fig. S9 of the Supplemental Material), and (iii) the steep energy dependence of the DOS at both edges of the pseudogap (Fig. 4) suggest that both the synthesis conditions and the superconducting properties may be further improved by adjusting the doping level and/or trying out different combinations of guests.

VI. CONCLUSIONS

In this work we performed a broad-range study of the thermodynamic stability and superconducting properties of X-doped B-C clathrates XB_3C_3. These compounds, recently synthesized under high pressure, are structurally related to the record-breaking cagelike superhydrides like LaH_{10} and YH_6, while their bonding and electronic properties, determined by the covalent B-C sublattice, are analogous to those of borides and carbides like MgB_2 and doped diamond [13,46]. Based on a full scan of the periodic table, we find that only five elements (Ca, Sr, Y, Ba, and La) form stable XB_3C_3 compounds at ambient or moderate pressure. Two of them (La, Sr) have already been experimentally synthesized [23,31,33]. While the superconducting T_c of ternary XB_3C_3 compounds are comparable to those of MgB_2, the best conventional superconductor known so far, ordered alloys XYB_6C_6 containing mono- and divalent elements are, instead, expected to yield a substantial improvement, reaching T_c's as high as 77 K. $KCaB_6C_6$ and $NaSrB_6C_6$, where a high T_c coexists with a relatively moderate stabilization pressure (20 and 18 GPa), represent very promising combinations of elements among all same- and inter-row combinations considered here. Our results also suggest that a careful tuning of dopants and compositions may prove chemically very feasible, and further increase T_c and/or reduce the stabilization pressure.

Note added. Recently, we became aware of another study on superconductivity in doped XB_3C_3 compounds; its main results are in excellent agreement with ours [48].

ACKNOWLEDGMENTS

The authors acknowledge support from Fondo Ateneo-Sapienza 2017-2019. The computational resources were provided by CINECA through Project No. IsC90-HTS-TECH_C, the Vienna Scientific Cluster (VSC) through Project No. P30269-N36 (Superhydra), and the dCluster of the Graz University of Technology. We thank A. Sanna for kindly sharing the code to numerically solve the isotropic Éliashberg equations.

[1] E. Snider, N. Dasenbrock-Gammon, R. McBride, M. Debessai, H. Vindana, K. Vencatasamy, K. V. Lawler, A. Salamat, and R. P. Dias, Nature (London) **586**, 373 (2020).

[2] A. P. Drozdov, M. E. M. I., I. Troyan, V. Ksenofontov, and S. Shylin, Nature (London) **525**, 73 (2015).

[3] D. Duan, Y. Liu, F. Tian, D. Li, X. Huang, Z. Zhao, H. Yu, B. Liu, W. Tian, and T. Cui, Sci. Rep. **4**, 6968 (2014).

[4] D. V. Semenok, I. A. Kruglov, I. A. Savkind, A. G. Kvashnin, and A. R. Oganov, Curr. Opin. Solid State Mat. Sci. **24**, 100808 (2020).

[5] T. Bi, N. Zarifi, T. Terpstra, and E. Zurek, Reference Module in Chemistry, Molecular Sciences and Chemical Engineering (2019), doi: 10.1016/B978-0-12-409547-2.11435-0.

[6] L. Boeri and G. B. Bachelet, J. Phys.: Condens. Matter **31**, 234002 (2019).

[7] C. J. Pickard, I. Errea, and M. I. Eremets, Annu. Rev. Condens. Matter Phys. **11**, 57 (2020).

[8] J. A. Flores-Livas, L. Boeri, A. Sanna, G. Profeta, R. Arita, and M. I. Eremets, Phys. Rep. **856**, 1 (2020).

[9] A. Sanna, C. Pellegrini, and E. K. U. Gross, Phys. Rev. Lett. **125**, 057001 (2020).

[10] L. Boeri, R. G. Hennig, P. J. Hirschfeld, G. Profeta, A. Sanna, E. Zurek, W. E. Pickett, M. Amsler, R. Dias, M. Eremets, C. Heil, R. Hemley, H. Liu, Y. Ma, C. Pierleoni, A. Kolmogorov, N. Rybin, D. Novoselov, V. I. Anisimov, A. R. Oganov *et al.*, J. Phys.: Condens. Matter **33** (2021), doi: 10.1088/1361-648X/ac2864.

[11] W. Chen, D. V. Semenok, X. Huang, H. Shu, X. Li, D. Duan, T. Cui, and A. R. Oganov, Phys. Rev. Lett. **127**, 117001 (2021).

[12] S. di Cataldo, C. Heil, W. von der Linden, and L. Boeri, Phys. Rev. B **104**, L020511 (2021).

[13] J. Nagamatsu, N. Nakagawa, T. Muranaka, Y. Zenitani, and J. Akimitsu, Nature (London) **410**, 63 (2001).

[14] J. M. An and W. E. Pickett, Phys. Rev. Lett. **86**, 4366 (2001).

[15] L. Boeri, J. Kortus, and O. K. Andersen, Phys. Rev. Lett. **93**, 237002 (2004).

[16] H. Rosner, A. Kitaigorodsky, and W. E. Pickett, Phys. Rev. Lett. **88**, 127001 (2002).

[17] M. Calandra, N. Vast, and F. Mauri, Phys. Rev. B **69**, 224505 (2004).

[18] A. N. Kolmogorov and S. Curtarolo, Phys. Rev. B **73**, 180501(R) (2006).

[19] J. E. Moussa and M. L. Cohen, Phys. Rev. B **77**, 064518 (2008).

[20] G. Savini, A. C. Ferrari, and F. Giustino, Phys. Rev. Lett. **105**, 037002 (2010).

[21] A. Jay, O. H. Duparc, J. Sjakste, and N. Vast, J. Appl. Phys. **125**, 185902 (2019).

[22] S. Saha, S. di Cataldo, M. Amsler, W. von der Linden, and L. Boeri, Phys. Rev. B **102**, 024519 (2020).

[23] L. Zhu, G. M. Borstad, H. Liu, P. A. Guńka, M. Guerette, J.-A. Dolyniuk, Y. Meng, E. Greenberg, V. B. Prakapenka, B. L. Chaloux, A. Epshteyn, R. E. Cohen, and T. A. Strobel, Sci. Adv. **6**, eaay8361 (2020).

[24] A. P. Drozdov, V. Minkov, S. Besedin, P. Kong, M. Kuzovnikov, D. Knyazev, and M. Eremets, arXiv:1808.07039.

[25] Z. M. Geballe, H. Liu, A. K. Mishra, M. Ahart, M. Somayazulu, Y. Meng, M. Baldini, and R. J. Hemley, Angew. Chem., Int. Ed. **57**, 688 (2018).

[26] A. P. Drozdov, P. P. Kong, V. S. Minkov, S. P. Besedin, M. A. Kuzovnikov, S. Mozaffari, L. Balicas, F. F. Balakirev, D. E. Graf, V. B. Prakapenka, E. Greenberg, D. A. Knyazev, M. Tkacz, and M. I. Eremets, Nature **569**, 528 (2019).

[27] H. Wang, J. S. Tse, K. Tanaka, T. Iitaka, and Y. Ma, Proc. Natl. Acad. Sci. **109**, 6463 (2012).

[28] F. Peng, Y. Sun, C. J. Pickard, R. J. Needs, Q. Wu, and Y. Ma, Phys. Rev. Lett. **119**, 107001 (2017).

[29] C. Heil, S. di Cataldo, G. B. Bachelet, and L. Boeri, Phys. Rev. B **99**, 220502(R) (2019).

[30] L. Zhu, T. A. Strobel, and R. E. Cohen, Phys. Rev. Lett. **125**, 127601 (2020).

[31] T. A. Strobel, L. Zhu, P. A. Guńka, G. M. Borstad, and M. Guerette, Angew. Chem., Int. Ed. **60**, 2877 (2021).

[32] L. Zhu, H. Liu, M. Somayazulu, Y. Meng, P. Guńka, T. B. Shiell, C. Kenney-Benson, S. Chariton, V. B. Prakapenka, H. Yoon, J. A. Horn, J. Paglione, R. Hoffmann, R. E. Cohen, and T. A. Strobel, arXiv:1708.03483.

[33] J.-N. Wang, X.-W. Yan, and M. Gao, Phys. Rev. B **103**, 144515 (2021).

[34] Computational details can be found in Sec. II.

[35] P. Giannozzi, S. Baroni, N. Bonini, M. Calandra, R. Car, C. Cavazzoni, D. Ceresoli, G. L. Chiarotti, M. Cococcioni, I. Dabo, A. D. Corso, S. de Gironcoli, S. Fabris, G. Fratesi, R. Gebauer, U. Gerstmann, C. Gougoussis, A. Kokalj, M. Lazzeri, L. Martin-Samos *et al.*, J. Phys.: Condens. Matter **21**, 395502 (2009).

[36] P. Giannozzi, O. Andreussi, T. Brumme, O. Bunau, M. B. Nardelli, M. Calandra, R. Car, C. Cavazzoni, D. Ceresoli, M. Cococcioni, N. Colonna, I. Carnimeo, A. D. Corso, S. de Gironcoli, P. Delugas, R. A. DiStasio, A. Ferretti, A. Floris, G. Fratesi, G. Fugallo *et al.*, J. Phys.: Condens. Matter **29**, 465901 (2017).

[37] D. R. Hamann, Phys. Rev. B **88**, 085117 (2013).

[38] J. P. Perdew, K. Burke, and M. Ernzerhof, Phys. Rev. Lett. **77**, 3865 (1996).

[39] M. Methfessel and A. T. Paxton, Phys. Rev. B **40**, 3616 (1989).

[40] S. Baroni, S. de Gironcoli, A. Dal Corso, and P. Giannozzi, Rev. Mod. Phys. **73**, 515 (2001).

[41] For all elements, we considered the ground-state structures under pressure, reported in literature; when the structures were not available, we employed structures predicted by evolutionary algorithsm (USPEX).

[42] See Supplemental Material at http://link.aps.org/supplemental/10.1103/PhysRevB.105.064516 for additional information on the structural, electronic, and vibrational properties of the structures discussed in the article.

[43] M. Aykol, S. S. Dwaraknath, W. Sun, and K. A. Persson, Sci. Adv. **4**, eaaq0148 (2018).

[44] In Fig. 3 we included ScB_3C_3, which is dynamically unstable (ferroelectric [30]), and YB_3C_3 and LaB_3C_3, which are insulators, to highlight and test the validity and limits of the rigid-band picture in this class of compounds.

[45] Specifically, since the top of the valence bands is threefold degenerate, we used the average of the square modulus of the wave functions belonging to this degenerate manifold.

[46] E. A. Ekimov, V. A. Sidorov, E. D. Bauer, N. N. Mel'nik, N. J. Curro, J. D. Thompson, and S. M. Stishov, Nature (London) **428**, 542 (2004).

[47] Dynamical instabilities result in small regions of imaginary frequencies in the phonon spectra of a few XYB_6C_6 compounds, which however do not spoil the overall agreement among them.

[48] P. Zhang, X. Li, X. Yang, H. Wang, H. Liu, and Y. Yao, arXiv:2108.11026.